High Resolution IR Spectroscopy: A Laboratory Program in Support of Planetary Atmospheric Research

T. Hewagama (U. of Maryland), W. E. Blass (U. of Tennessee),
T. Kostiuk (NASA/GSFC), J. Delgado (U. of Maryland)

ABSTRACT

We report on our molecular spectroscopy effort to determine frequencies, intensities, shapes and broadening in fundamental and low-lying hot band transitions for molecules of interest to contemporary planetary atmospheric investigations in NASA's Planetary Atmospheres Program. We identified molecular species of significance to NASA's Cassini Mission to Jupiter, Saturn and Titan: ethane, including both normal and primary hot band; ethylene; and allene. The interpretation of ethane emission from the atmospheres of Jupiter, Saturn and Titan has presented difficulties. We attribute these modeling difficulties to errors and incompleteness in the line atlas source.

High spectral resolution (0.00003 cm-1 at 12 microns) laboratory measurements, obtained with the NASA/GSFC Heterodyne Instrument for Planetary Wind and Composition (HIPWAC) instrument, were the basis of spectroscopic results reported herein. The HIPWAC instrument (Fig. 1) and measurements are described in a companion paper (Blass et al., 2008) in this session. At these spectral resolutions, the rotation-vibration transitions measured under laboratory conditions (ambient temperature and ~1 Torr pressure) are fully resolved and identified without ambiguity. The principal objective is to provide critical laboratory truth for the interpretation of infrared spectral observations of the Cassini mission and in the re-interpretation of mid-IR emission spectra from Voyager IRIS, ISO and ground based IR data of the outer planets. We discuss the analysis methodology and interpretation of the HIPWAC laboratory measurements, and compare to results of other researchers.

Heterodyne Instrument for Planetary Wind and Composition (HIPWAC)

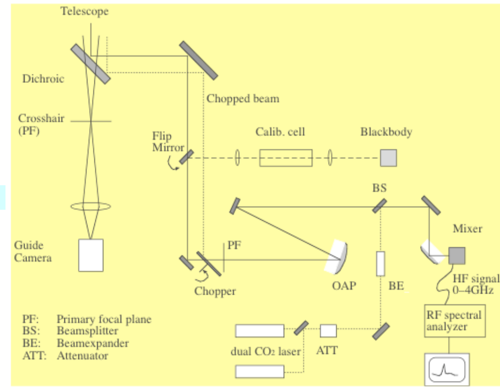

Fig. 1

SIGNIFICANCE

We identified molecular species of significance to NASA's Cassini Mission to Jupiter, Saturn and Titan: ethane (C_2H_6), including both normal and primary hot band (*i.e.*, ν_9 and $\nu_9+\nu_4-\nu_4$); ethylene (C_2H_4); and allene (C_3H_4). The laboratory measurements which are the basis for the results reported herein were obtained at a spectral resolution of 0.00003 cm^{-1} (~1MHz) at 12µm. At this spectral resolution, the rotation-vibration transitions measured under laboratory conditions (ambient temperature and ~1 Torr pressure) are fully resolved and identified without ambiguity. The principal objective is to provide critical laboratory truth for the interpretation of IR spectral observations of the Cassini mission and in the reinterpretation of mid-IR emission spectra from Voyager IRIS, ISO and ground based IR data of the outer planets.

LABORATORY SPECTROSCOPY ANALYSIS FACILITY

We developed an IDL based facility for the analysis of high resolution Voigt line shaoe data from different spectroscopic instruments. The facility calibrates and removes instrument effects that could introduce systematic errors which decrease the precision level in recovering weaker lines. The facility includes a combination of options for extracting spectroscopic parameters (e.g., derive a common value for the widths of bandpass lines; fix the Doppler width and Voigt parameter) and extracts parameters such as line strength, frequency, and width using a non-linear Levenberg-Marquardt based optimization. Analysis of HIPWAC measurements of ethane, allene, and ethylene involve spectra with $\nu/\Delta\nu>10^7$ and provide the ability to recover transition frequencies to better than a part in 10^8. Spectral resolution is better (smaller) than 1 MHz for room temperature Doppler broadened lines with a room temperature HWHM of ~30 MHz and the spectral lines are fully resolved! This allows for very accurate recovery of molecular spectroscopic parameters such as the transition frequency and intensity. A careful examination of gas cell temperature and pressure is included in error estimates of derived spectroscopic parameters.

ETHANE RESULTS

The ν_9 band region of ethane, near 12.2 µm is among the most ubiquitous and prominent emission features in the thermal IR spectrum of the outer solar system bodies such as Jupiter, Saturn, Titan and Neptune. An illustrative case is the analysis of Jupiter and Titan atmospheric ethane (C_2H_6) ν_9 band emission observed by Cassini/CIRS – which have a bearing on the atmospheric thermal structure and photochemistry constraints. While researchers are able to model the acetylene (C_2H_2) spectra to a high precision (few percent), the ethane spectra show much larger residuals (~15% level in the lines and a broad structure near the 845 cm^{-1} portion of the band; C.Nixon, personal communication). We attribute these differences to hot band lines which are sensitive to temperature and consequently serve as probes of the line formation region. Ideally, any modeling of spectral regions with fundamental bands of complex molecules should incorporate these temperature-dependent contributions. We have used the HIPWAC measurements of C_2H_6 to improve our ethane torsional model and generate high accuracy predictions for line centers and intensities. Delgado *et al.* (this session) show the impact of using such spectroscopic parameters in the analysis of Titan ethane observations with comparable spectral resolution. The inclusion of missing spectral lines has the potential to resolve modeling difficulties of observations of ethane in outer planet atmospheres.

An example spectrum and fit are shown in Fig. 2, and a our results are summarized n Table 1. Our new atlas has been intensity corrected against the best 12 spectral lines shown in the table, and the absolute frequency and intensities retrievals are better than 1MHz (0.00003 cm-1) and 5%, respectively. Recently, Vander Auwera et al. [2] published an atlas of ethane spectroscopic parameters that have resolved some of the modeling anomalies. Our results, which are based on fully resolved spectral lines are in good agreement with Vander Auwera et al. [2] for the strong lines, but also include several measured weaker lines that are spectroscopically identified and characterized for the first time. Our ability to measure weak lines leads to better constraints on the ethane band intensity (Table 2).

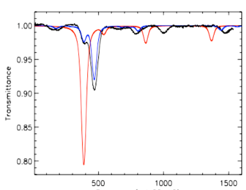

Fig. 2: shows an example HIPWAC laboratory spectrum of C_2H_6 (black trace) near the P18 (851.50514 cm^{-1}) $^{14}C^{16}O_2$ laser transition. The blue and red curves are spectra calculated using the molecular spectroscopic parameters in the previous version of the Univ. of Tennessee and current HITRAN line atlases, respectively. The spectral measurements were made with a 30 cm long cell filled to a pressure of 0.71 Torr with ethane.

TABLE 1
Measured parameters
TN/GSFC atlas (TN/G2007)
Vander Auwera et al. 2007 atlas
(Auwera)

	Assignment ΔKΔϑK,ϑ,σ	Measured cm^-1	TN/G2007 cm^-1	List2-Auwera cm^-1	HITRAN cm^-1	Meas Δν(MHz)	TN-G-07 Δν(MHz)	Measured intensity	HITRAN intensity	TN-G-07 intensity	LIST2-Auwer intensity
		858.1583905									
	RR(6,14,0)	858.1101064	858.11	858.11006	858.1057	-1448	-1452	5.94E-22	2.09E-21	6.01E-22	6.40E-22
	RR(6,14,2)	858.1064292	858.1065	858.10634	858.0852	-1558	-1555	3.00E-22	2.09E-21	3.00E-22	3.20E-22
P12		856.515448									
	PR(4,34,2)	856.530507	856.5333	N/A		451	535	9.96E-24		3.19E-23	N/A
	RR(4,17,0)	856.4842025	856.4838	856.48414		-937	-948	1.04E-22		1.21E-22	1.29E-22
	RR(4,17,2)	856.4790288	856.4792	856.47905	856.4802	-1092	-1086	4.72E-22	2.09E-21	4.82E-22	5.14E-22
	PR(4,34,0)	856.557511	856.5572	N/A		1261	1253	3.17E-23		7.98E-24	N/A
P14		854.8563139									
	RQ(12,19,2)	854.8650441	854.865	854.86453		262	260	6.35E-23		4.52E-23	4.84E-23
	RQ(12,19,0)	854.8683818	854.8681	854.8678		362	354	1.02E-22		9.04E-23	9.68E-23
	RQ(12,20,0)	854.8139082	854.8138	854.81356		-1271	-1275	9.40E-23		8.91E-23	9.55E-23
	RQ(12,20,2)	854.8104008	854.8105	854.8101		-1376	-1373	7.13E-23		4.46E-23	4.78E-23
P16		853.180996									
	RQ(12,40,2)	853.1780981	853.1781	853.17422		-87	-86	-3.44E-24		2.53E-24	2.79E-24
	PR(1,25,3)	853.1579544	853.1597	853.15802		-691	-637	5.08E-23		5.19E-23	5.58E-23
	RR(7,8,1)	853.1212927	853.1212	853.12119	853.1172	-1790	-1792	8.02E-22	2.09E-21	8.17E-22	8.62E-22
	RR(7,8,3)	853.118942	853.1189	853.11884		-1860	-1862	2.40E-22		2.04E-22	2.15E-22
		851.489499									
	PR(6,34,0)	851.4959617	851.4951	N/A		194	167	4.21E-23		2.23E-23	N/A
P18	RR(5,11,3)	851.5024852	851.5023	851.50232		389	385	1.45E-22		1.79E-22	1.89E-22
	RR(5,11,1)	851.5051619	851.5051	851.50503	851.5024	470	467	6.83E-22	2.09E-21	7.16E-22	7.54E-22
	RQ(11,27,1)	851.5159022	851.5163	851.51515		792	803	8.71E-23		6.70E-23	7.21E-23
	RQ(11,28,1)	851.4404217	851.4415	851.4403		-1471	-1439	5.21E-23		5.89E-23	6.34E-23
	RQ(11,28,3)	851.4375604	851.4373	851.43687		-1557	-1566	2.25E-23		1.47E-23	1.59E-23
	PR(5,32,3)	851.5447719	851.5458	N/A		1657	1687	-4.96E-25		9.53E-24	N/A
	PR(5,32,1)	851.5603253	851.5592	N/A		2123	2089	3.57E-23		3.81E-23	N/A
		848.0579728									
	RQ(10,35,0)	848.0329389	848.0328	848.03149		-750	-755	3.92E-23		5.86E-24	6.36E-24
P22	PR(2,23,2)	848.0871906	848.0879	848.08711		876	896	2.59E-22		2.09E-22	2.22E-22
	PR(2,23,0)	848.0974171	848.098	848.09713	848.0916	1183	1200	5.36E-23	2.09E-21	5.23E-23	5.57E-23
	PR(3,25,1)	848.0106511	848.0116	848.0107		-1419	-1391	8.36E-23		7.16E-23	7.63E-23
	PR(3,25,3)	848.0037379	848.0036	848.00386	848.0098	-1626	-1629	1.51E-22	2.09E-21	1.43E-22	1.53E-22
	RP(22,27,0)	848.1154359	848.1164	N/A		1723	1750	9.04E-23		6.93E-27	N/A
	RQ(10,34,2)	848.1178292	848.1167	848.11496		1794	1760	8.45E-23		2.83E-23	3.07E-23
	RQ(10,34,0)	848.1239191	848.1241	848.12291		1977	1982	3.61E-23		7.08E-24	7.68E-24
		846.3179398									
	RR(5,7,1)	846.3156121	846.3155	846.31563		-70	-73	7.70E-22		8.20E-22	8.56E-22
	RR(5,7,3)	846.3130983	846.3131	846.31322		-145	-145	3.12E-22		2.05E-22	2.14E-22
P24	RQ(9,20,3)	846.3246914	846.3248	846.32436	846.3257	202	204	2.11E-22	2.09E-21	2.08E-22	2.20E-22
	RQ(9,20,1)	846.3277785	846.3281	846.32738		295	303	1.10E-22		1.04E-22	1.10E-22
	RQ(9,21,1)	846.2718449	846.2723	846.27162		-1382	-1368	8.53E-23		9.77E-23	1.04E-22
	RQ(9,21,3)	846.2688405	846.2689	846.26851		-1472	-1471	2.51E-22		1.95E-22	2.07E-22
	RQ(9,19,3)	846.3778653	846.3779	846.37761		1797	1799	2.62E-22		2.19E-22	2.31E-22
	RQ(9,19,1)	846.380833	846.3811	846.38054		1885	1894	1.29E-22		1.09E-22	1.16E-22
		842.7892987									
	RQ(8,31,2)	842.7846426	842.7853	842.78419		-140	-119	6.98E-23		7.16E-23	7.66E-23
P28	PR(8,31,2)	842.7807998	842.7806	N/A		-255	-262	4.00E-24		2.37E-23	N/A
	PR(7,29,1)	842.8207941	842.8184	842.82055		944	873	4.84E-23		4.00E-23	4.26E-23
	PR(9,33,3)	842.7550584	842.7559	N/A		-1027	-1003	2.65E-23		1.35E-23	N/A
	RQ(8,30,2)	842.864851	842.8656	842.86453		2265	2288	1.24E-22		8.41E-23	8.98E-23
	RQ(8,32,0)	842.7115719	842.7103	842.70973		-2330	-2368	3.74E-23		1.51E-23	1.62E-23
		841.0006684									
	RQ(7,15,1)	840.9943093	840.9945	840.99421	840.991	-191	-186	3.81E-22	2.09E-21	3.76E-22	3.92E-22
	RQ(7,15,3)	840.9914478	840.9916	840.99142		-276	-272	1.23E-22		9.40E-23	9.81E-23
	RR(4,5,0)	840.9791499	840.9788	840.97906		-645	-655	1.60E-22		1.97E-22	2.04E-22
P30	RR(4,5,2)	840.9766554	840.9764	840.97662		-720	-726	8.07E-22		7.86E-22	8.14E-22
	RQ(7,14,3)	841.0311323	841.0312	841.03097		913	914	8.58E-23		9.26E-23	9.66E-23
	RQ(7,14,1)	841.0339126	841.034	841.03368		997	998	3.83E-22		3.70E-22	3.86E-22
	RQ(7,16,1)	840.9522602	840.9526	840.95216		-1451	-1443	3.39E-22		3.74E-22	3.91E-22
	RQ(7,16,3)	840.9493088	840.9495	840.94927		-1540	-1533	7.70E-23		9.36E-23	9.77E-23
	RQ(8,49,2)	841.0553689	840.9453	N/A		1640	-1661	2.74E-24		1.11E-24	N/A
	RQ(7,13,3)	841.0681287	841.0681	841.06794		2022	2020	4.70E-23		8.90E-23	9.28E-23
	RQ(7,13,1)	841.0708533	841.0708	841.07056		2104	2101	3.01E-22		3.56E-22	3.71E-22
		839.1958112									
	PR(3,18,1)	839.1893179	839.1896	839.18923	839.1899	-195	-186	1.64E-22	2.09E-21	1.26E-22	1.32E-22
P32	RR(0,12,2)	839.1820314	839.1821	N/A		-413	-412	1.44E-22		1.75E-22	N/A
	PR(2,16,2)	839.2303144	839.2304	839.23007	839.2344	1034	1038	3.25E-22	2.09E-21	3.31E-22	3.44E-22
	PR(4,20,0)	839.1582923	839.1579	839.15839		-1125	-1137	5.39E-23		4.65E-23	4.87E-23
	PR(2,16,0)	839.236928	839.2366	839.2367		1233	1223	1.13E-22		8.27E-23	8.62E-23
	PR(4,20,2)	839.1480996	839.1482	839.14812	839.1377	-1430	-1427	1.90E-22	2.09E-21	1.86E-22	1.95E-22
	PR(5,22,1)	839.1233561	839.1235	839.12355		-2172	-2168	1.14E-22		1.31E-22	1.38E-22

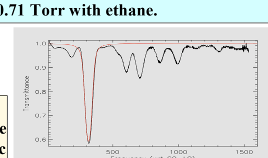

Fig. 3: shows the allene spectrum near 858.1479 cm^{-1} measured at 0.00003 cm^{-1} spectral resolution (black trace) and a model (red trace) calculated with molecular spectroscopic parameters from Wang *et al.* [3].

ALLENE RESULTS

We have also been improving the allene atlas using the HIPWAC measurements of allene. Fig. 3 is an example allene measurement at a spectral resolution of 0.00003 cm^{-1} compared to a model we calculated using the spectroscopic parameters given by Wang *et al.* [3]. When the model was scaled to match the measured halfwidth, we find excellent agreement for the strong line. Since Wang *et al.* [3] used a lower spectral resolution in their study it is likely the lower intensity lines were not measured with sufficient precision. However, the agreement in the strong line is a good validation of our analysis tools. We are using our analysis tools to recover and characterize spectroscopic parameters for the higher density weaker lines. The contributions from allene, which overlap the ethane band, may also be a part of the puzzle in the interpretation of the spectroscopy of outer planet atmospheres.

TABLE 2.

	T(K)	$S(\nu_9)$ 10^{-19} cm/mol	$S(RQ_0)$ 10^{-19} cm/mol
ATMOS 1995	296	6.967	0.253
GEISA 2003	296	5.743	0.229
HITRAN 2004	296	14.56	0.571
AUWERA LIST 3	296	7.548	0.261
TN/G2007 (THIS WORK)	296	6.941	0.270

REFERENCES

[1] Blass W. E., Delgado J., Kostiuk T., and Hewagama T., *see companion paper in this session* (2008).
[2] Vander Auwera J., Moazzen-Ahmadi N. and Flaud J.-M. (2007) *ApJ, 662*, 750–757.
[3] Wang W. F., Sirota J. M., and Reuter D. C. (1999) *J. Mol. Spec., 194*, 256-268.

The authors gratefully acknowledge the NASA Planetary Atmospheres Program for supporting this research.